

RESEARCH ARTICLE

# A monomethyl auristatin E-conjugated antibody to guanylyl cyclase C is cytotoxic to target-expressing cells *in vitro* and *in vivo*

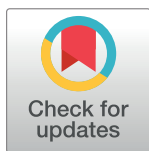
Melissa Gallery<sup>1</sup>\*, Julie Zhang<sup>2</sup>\*, Daniel P. Bradley<sup>3</sup>, Pamela Brauer<sup>4</sup>, Donna Cvet<sup>3</sup>, Jose Estevam<sup>5</sup>, Hadi Danaee<sup>5</sup>, Edward Greenfield<sup>4a</sup>, Ping Li<sup>4</sup>, Mark Manfredi<sup>2</sup>, Huay-Keng Loke<sup>6</sup>, Claudia Rabino<sup>1</sup>, Brad Stringer<sup>7</sup>, Mark Williamson<sup>8</sup>, Tim Wyant<sup>9</sup>, Johnny Yang<sup>10</sup>, Qing Zhu<sup>10</sup>, Adnan Abu-Yousif<sup>2</sup>, O. Petter Veiby<sup>11\*</sup>

**1** Molecular & Cellular Oncology, Millennium Pharmaceuticals, Inc., a wholly owned subsidiary of Takeda Pharmaceutical Company Limited, Cambridge, MA, United States of America, **2** Cancer Pharmacology, Millennium Pharmaceuticals, Inc., a wholly owned subsidiary of Takeda Pharmaceutical Company Limited, Cambridge, MA, United States of America, **3** Biomedical Imaging, Millennium Pharmaceuticals, Inc., a wholly owned subsidiary of Takeda Pharmaceutical Company Limited, Cambridge, MA, United States of America, **4** Protein Sciences, Millennium Pharmaceuticals, Inc., a wholly owned subsidiary of Takeda Pharmaceutical Company Limited, Cambridge, MA, United States of America, **5** Biomarker Assay & Exploratory Biology, Millennium Pharmaceuticals, Inc., a wholly owned subsidiary of Takeda Pharmaceutical Company Limited, Cambridge, MA, United States of America, **6** Oncology Biochemistry, Millennium Pharmaceuticals, Inc., a wholly owned subsidiary of Takeda Pharmaceutical Company Limited, Cambridge, MA, United States of America, **7** Molecular Pathology, Millennium Pharmaceuticals, Inc., a wholly owned subsidiary of Takeda Pharmaceutical Company Limited, Cambridge, MA, United States of America, **8** US Medical Affairs, Millennium Pharmaceuticals, Inc., a wholly owned subsidiary of Takeda Pharmaceutical Company Limited, Cambridge, MA, United States of America, **9** Translational Medicine, Millennium Pharmaceuticals, Inc., a wholly owned subsidiary of Takeda Pharmaceutical Company Limited, Cambridge, MA, United States of America, **10** DMPK, Millennium Pharmaceuticals, Inc., a wholly owned subsidiary of Takeda Pharmaceutical Company Limited, Cambridge, MA, United States of America, **11** Global Biotherapeutics, Millennium Pharmaceuticals, Inc., a wholly owned subsidiary of Takeda Pharmaceutical Company Limited, Cambridge, MA, United States of America

\* These authors contributed equally to this work.

✉ Current address: Dana-Farber Cancer Institute, Boston, MA, United States of America

\* [Petter.Veiby@takeda.com](mailto:Petter.Veiby@takeda.com)



**OPEN ACCESS**

**Citation:** Gallery M, Zhang J, Bradley DP, Brauer P, Cvet D, Estevam J, et al. (2018) A monomethyl auristatin E-conjugated antibody to guanylyl cyclase C is cytotoxic to target-expressing cells *in vitro* and *in vivo*. PLoS ONE 13(1): e0191046. <https://doi.org/10.1371/journal.pone.0191046>

**Editor:** Hiroshi Shiku, Mie University Graduate School of Medicine, JAPAN

**Received:** June 15, 2017

**Accepted:** December 27, 2017

**Published:** January 25, 2018

**Copyright:** © 2018 Gallery et al. This is an open access article distributed under the terms of the [Creative Commons Attribution License](https://creativecommons.org/licenses/by/4.0/), which permits unrestricted use, distribution, and reproduction in any medium, provided the original author and source are credited.

**Data Availability Statement:** All relevant data are within the paper and its Supporting Information files.

**Funding:** This study was funded by Takeda Pharmaceuticals International Co. Moreover, Takeda Pharmaceuticals (<https://www.takeda.com/>) provided support in the form of salaries for authors (MG, JZ, DPB, PB, DC, JE, HD, EG, PL, MM, HKL, CR, BS, MW, TW, JY, QZ, AAY, and OPV) but did not have any additional role in the

## Abstract

Guanylyl cyclase C (GCC) is a cell-surface protein that is expressed by normal intestinal epithelial cells, more than 95% of metastatic colorectal cancers (mCRC), and the majority of gastric and pancreatic cancers. Due to strict apical localization, systemically delivered GCC-targeting agents should not reach GCC in normal intestinal tissue, while accessing antigen in tumor. We generated an investigational antibody-drug conjugate (TAK-264, formerly MLN0264) comprising a fully human anti-GCC monoclonal antibody conjugated to monomethyl auristatin E via a protease-cleavable peptide linker. TAK-264 specifically bound, was internalized by, and killed GCC-expressing cells *in vitro* in an antigen-density-dependent manner. In GCC-expressing xenograft models with similar GCC expression levels/patterns observed in human mCRC samples, TAK-264 induced cell death, leading to tumor regressions and long-term tumor growth inhibition. TAK-264 antitumor activity was generally antigen-density-dependent, although some GCC-expressing tumors were

study design, data collection and analysis, decision to publish, or preparation of the manuscript.

**Competing interests:** All authors were employees of Millennium Pharmaceuticals, Inc., a wholly owned subsidiary of Takeda Pharmaceutical Company Limited, at the time this work was conducted. This does not alter our adherence to PLOS ONE policies on sharing data and materials.

refractory to TAK-264-targeted high local concentrations of payload. These data support further evaluation of TAK-264 in the treatment of GCC-expressing tumors.

## Introduction

Gastrointestinal cancers are among the most common cancers in the United States, with an estimated 291,150 new cases of digestive system cancers in 2015; notably, colon/rectum and pancreatic cancers are the third and fourth most common causes of cancer-related deaths, with an estimated 49,700 and 40,560 deaths, respectively, in 2015 [1]. Prognosis is poor with many gastrointestinal malignancies; for example, approximately one fifth of patients with colorectal cancer (CRC) have distant metastases [2–5]. Current chemotherapeutic options for metastatic CRC (mCRC) include combination chemotherapies and molecularly targeted monoclonal antibody therapies [6]; however, although treatment options are expanding, 5-year survival for patients with distant metastases is only approximately 10% [5–7]. Similarly, median survival for patients with pancreatic cancer is only 4–6 months [8]. Clearly, investigations into new treatment strategies are warranted.

Guanylyl cyclase C (GCC) is a transmembrane cell surface receptor that functions in the maintenance of intestinal fluid, electrolyte homeostasis, and restriction of cell proliferation [9]. In normal human tissues, GCC expression is restricted to the mucosal cells lining the small intestine, large intestine, and rectum [10, 11]. GCC expression is maintained upon neoplastic transformation of intestinal epithelial cells, with expression in >95% of primary and metastatic colorectal tumors [10, 12–14] and in 60–70% of gastric, esophageal, and pancreatic cancers [15–17]. The tissue-restricted expression and consistent association with CRC has been exploited for use of GCC as a diagnostic and prognosis marker for this disease [10, 14, 18–20]. Recent studies have suggested GCC expression is a marker of therapeutic response in mCRC [11].

In normal intestinal tissue, GCC is expressed on the apical side of epithelial cell tight junctions that form an impermeable barrier between the luminal environment and vascular compartment [21, 22]. As such, systemic intravenous administration of a therapeutic anti-GCC antibody should not affect normal intestinal GCC receptors, while having access to extraintestinal GCC-expressing tumors. The selective targeting of colon tumor cells with GCC ligands has been demonstrated *in vivo* [23, 24]. In one study, a radionuclide-conjugated GCC ligand was shown to selectively target GCC-expressing colon tumor xenografts in mice, with no accumulation in the normal mouse intestinal epithelium [24]. Similarly, formation of metastases was significantly reduced in mouse models of mCRC through immunization with GCC-expressing viral vectors with no evidence of autoimmunity [25]. Additionally, GCC internalizes through receptor-mediated endocytosis upon ligand binding, making it a candidate for intracellular delivery of anticancer therapeutic proteins [14, 26].

Antibody-drug conjugates (ADCs) are an emerging therapeutic modality for the targeted delivery of potent cytotoxic agents to tumors [27, 28]. Recent developments have included the anti-CD30 ADC brentuximab vedotin [29, 30], which is approved in the USA and EU for the treatment of relapsed or refractory Hodgkin lymphoma and systemic anaplastic large cell lymphoma, and the human epidermal growth factor receptor 2 (HER2)-targeted ADC trastuzumab emtansine [31], which is approved in the USA and EU for the treatment of HER2-positive breast cancer. Many other ADCs are currently in clinical development, building upon these successes [32]; the attributes of GCC make it an enticing target for an ADC strategy.

TAK-264 (formerly MLN0264) is a novel ADC consisting of a fully human anti-GCC monoclonal antibody conjugated to the potent microtubule-disrupting agent monomethyl auristatin E (MMAE) via the protease-cleavable peptide maleimido-caproyl-valine-citrulline [vc]. MMAE and the linker technology are licensed from Seattle Genetics, Inc. In the present study, we demonstrate that TAK-264 binds to, is internalized by, and leads to dose-dependent, selective cell death and antitumor activity in GCC-expressing cells *in vitro* and *in vivo*, respectively. Thus, TAK-264 has potential for development as an ADC therapeutic in GCC-expressing tumors.

## Materials and methods

### Generation of GCC protein and anti-GCC antibodies

Recombinant protein containing the extracellular domain of human GCC fused to human immunoglobulin G (IgG1) Fc was used to immunize female C57BL/6 mice (Taconic Farms, Germantown, NY) or Xenomice (Abgenix, Fremont, CA), for the generation of hybridomas. Monoclonal antibodies were generated by fusing spleen cells and SP 2/0 myeloma cells (ATCC No. CRL8-006, Rockville, MD) with a polyethylene glycol 1450 (ATCC) fusion procedure [33]. Hybridoma supernatants were screened for anti-GCC antibodies using indirect ELISA and flow cytometry on GCC transfected HT-29 cells. Positive hybridomas were subcloned to achieve monoclonality.

Recombinant anti-GCC monoclonal antibody was prepared using molecular biology techniques to isolate the coding sequences for the variable regions from the hybridoma cell line and combine them with sequences for human IgG1 and human kappa constant regions in an in-house-generated expression vector, pTOK58D. CHO DG44 cells adapted to serum-free, suspension media were transfected with this expression construct using electroporation, selected with Geneticin (G418), amplified with methotrexate (MTX), and limited-dilution cloned to generate a high-producing cell line to support pre-clinical and phase 1 clinical studies. This cell line was shown to be stable, mycoplasma free, and bio-burden free, and was used for production of the anti-GCC monoclonal antibody, which was used for conjugation to MMAE to generate TAK-264.

For large-scale production of the unconjugated anti-GCC monoclonal antibody, the above-generated cell line was scaled up in serum-free, animal-component-free medium in bioreactors or biowave bags, fed every 3 days, and harvested when the viability was <40%. The supernatant underwent standard Protein A capture purification, concentration/diafiltration, and a final endotoxin cleanup using detoxigel. Concentration of the anti-GCC monoclonal antibody was determined using the formula  $(A_{280} - A_{320})/1.4$ , and endotoxin content was determined using the Pyrochrome<sup>®</sup> chromogenic test kit (Associates of Cape Cod). For conjugation purposes, the antibody was concentrated to 10 mg/mL, using Vivaspin 15 MWCO 30,000 kDa. The anti-GCC monoclonal antibody was conjugated to MMAE by Seattle Genetics according to previously published protocols. An average of 3.7 MMAE molecules were conjugated per antibody.

### Quantitative RT-PCR analysis of GCC in human tissues

Frozen human tissues for mRNA extraction were procured from ProteoGenex, Inc. (Culver City, CA, USA). Semi-quantitative reverse transcription polymerase chain reaction (RT-PCR) was undertaken using TaqMan<sup>®</sup> probe specific for GCC. Relative expression levels were normalized according to the expression of beta 2 microglobulin.

## Cell lines

All cell lines used in this study were generated internally at Millennium Pharmaceuticals, Inc., a wholly owned subsidiary of Takeda Pharmaceutical Company Limited. HEK293 cells (ATCC, Manassas, VA, USA) were maintained in 90% Dulbecco's Modified Eagle's Medium (DMEM, 11995–040, Invitrogen), 10% fetal bovine serum (FBS, SH 30071.02, Hyclone), 1% L-glutamine (25030–081, Invitrogen), and (HEK293-GCC cells) 10  $\mu\text{g}/\text{mL}$  of blasticidin (R21001, Invitrogen). All cells were grown at 37°C in a humidified atmosphere with 5%  $\text{CO}_2$ . The HEK293-vector cells were generated by using a vector named pN8 $\Phi\beta$ mycSV40 that was created by Millennium Pharmaceuticals. The HEK293-GCC cells were generated by cloning in the full-length GCC sequence into the same vector pN8 $\Phi\beta$ mycSV40. After confirmation by sequencing of pN8 $\Phi\beta$ mycSV40 human GCC DNA, the stable cell lines were generated by transfection with Lipofectamine 2000. Cells ( $2 \times 10^6$ ) were transfected with 24  $\mu\text{g}$  of DNA + 60  $\mu\text{L}$  of Lipofectamine 2000 in 1500  $\mu\text{L}$  of Opti-MEM each. The transfected cells were maintained in complete media for 48 h before changing to selection media for 2 weeks. Western blot analysis using anti-mouse GCC(3G1), as well as FACS analysis with anti-human GCC, confirmed the generation of stable cell lines expressing the control vectors or human GCC.

Cryopreserved early-passage cells were re-established in culture for all experiments. Transcriptional profiling of cell lines confirmed that vector control cell lines differed only in the expression level of GCC.

## Western blot analysis

Cells were collected and washed in Dulbecco's phosphate buffered saline (PBS) without  $\text{CaCl}_2$  and without  $\text{MgCl}_2$  (14190–144, Invitrogen) and spun down. For denaturing polyacrylamide gels, cell pellets were lysed in buffer containing 10 mM Tris (pH 7.5) with 1% Triton X-100, supplemented with protease inhibitor (complete-mini tablets, Roche), by three rounds of vortexing, and incubation on ice for 5 min. Lysates were cleared by centrifugation and the protein concentrations in the supernatants were determined using the Bradford assay. Equal amounts of total protein (50  $\mu\text{g}$ ) were denatured and loaded on 7% Tris-Acetate SDS-PAGE gels (EA 0358, Invitrogen), transferred to nitrocellulose membrane (Invitrogen), using Invitrogen's Tris-Acetate transfer buffer and XCell Blot Module for 1.5 h at 30 V. Membranes were blocked with 5% nonfat skim milk in Tris-buffered saline-Tween 20 (TBS-T) for 1 h at room temperature, washed with TBS-T and incubated for 3 h with primary antibodies (3G1 or an anti-actin goat polyclonal antibody [Santa Cruz Biotechnology]). After washing with TBS-T, membranes were incubated for 1 h with secondary antibodies (HRP-conjugated goat anti-mouse IgG [Perkin-Elmer] and donkey anti-goat IgG [Santa-Cruz Biotechnology], respectively). Blots were developed using enhanced chemiluminescence (Amersham, Piscataway, NJ).

## Cell surface binding assay

Antibody binding to cells was evaluated by an indirect immunofluorescence assay using flow cytometry.  $1 \times 10^6$  cells/well were plated in a V-bottom 96-well plate and incubated on ice for 1 h with serial antibody dilutions of 1–0.001  $\mu\text{g}/\text{mL}$ . Cells were washed twice with 3% FBS in ice-cold PBS and incubated with 1:200 mouse anti-human PE IgG (Southern Biotech 2043–09) for 1 h on ice. Cells were washed again and analyzed by flow cytometry on a Becton Dickinson FACScan flow cytometer. Data was analyzed using Winlist 4.0 Software (Verity Software House, Topsham, ME) and background-corrected mean fluorescence intensity was determined. Mean fluorescence intensities were plotted versus antibody concentration using Winlist 4.0 Software (Verity Software House, Topsham, ME).



## Antibodies for Western blot analysis and immunofluorescence

The anti-actin goat polyclonal (SC-1616) and anti-goat IgG (donkey) HRP secondary (SC-2056) were obtained from Santa Cruz Biotechnology. The anti-mouse IgG (goat) HRP-labeled secondary (NEF 822) was purchased from Perkin Elmer. For immunofluorescence, anti-GCC monoclonal antibodies were used as primaries and Alexa-fluor conjugated goat anti-human antibodies (Invitrogen) were used as secondary antibodies.

## Internalization assay

Cells were grown on coverslips and placed on ice for 10 min prior to adding antibody (TAK-264 10  $\mu\text{g}/\text{mL}$ ) in cold culture medium. Cells were maintained on ice for 20 min to allow cell surface binding by the antibody. For internalization, antibody-containing medium was replaced with fresh culture medium and cells were incubated at 37°C for 3 h. Control plates were kept on ice for the same length of time. Cells were briefly rinsed in PBS and fixed for 5 min in 4% paraformaldehyde at room temperature. Cells were subsequently washed in PBS, permeabilized for 15 min in 0.5% Triton X-100, and incubated in 0.5% blocking reagent (Roche, cat. #1095176) in 100 mM Tris-HCl pH 7.5, 150 mM NaCl. An appropriate dilution of Alexa Fluor<sup>®</sup> 488 conjugated secondary antibody (ThermoFisher Scientific) was made in 0.5% blocking reagent and added to the cells for 30 min at room temperature. Cells were then washed three times for 5 min in PBS. Coverslips were mounted on glass slides using Vecta Shield Mounting Medium (Vector Laboratories). Staining was visualized by laser scanning confocal microscopy (Zeiss Pascal) and analyzed using Axiovert software.

## Determination of MMAE concentration following TAK-264 *in vitro* and *in vivo*

For *in vitro* assessment, 4 million HEK293-GCC cells were seeded in complete media, into 10 cm<sup>2</sup> plates, 48 h prior to performing the experiment. On the day of experiment, media was carefully removed and cells were washed with 2 mL ice-cold media without FBS. Media was aspirated and 9 mL ice-cold media was added to each plate. Plates were placed on ice for 10 min, followed by addition of 1  $\mu\text{g}$  of ADC to each plate, and incubated at either 4°C or 37°C for the time indicated. For each condition, media was collected at the completion of the incubation time at 4°C or 37°C. Plates were washed with 1 mL PBS and scraped to remove adherent cells. Samples were collected and spun down in centrifuge tubes at 1000 rpm. Tubes containing cell culture supernatant and cell pellets were stored at -80°C, until analyzed.

MMAE in tumor samples was determined by extraction of the tumor and homogenizing in mouse plasma based on weight (1:4, equivalent weight in mg vs. plasma volume in  $\mu\text{L}$ ) on a FastPrep-24 homogenizer (MP Biomedicals, Solon, OH) for concentration analysis. Quantification of MMAE was conducted using a method based on liquid chromatography–tandem mass spectrometry (LC/MS/MS) methodology. A protein-precipitation method was used to extract MMAE from the bio-matrix. The internal standard used for analysis was a stable isotope-labeled MMAE. The dynamic range of the assay was 0.02–50 ng/mL.

## *In vitro* cytotoxicity assay

HEK293-vector and HEK293-GCC cells were plated in 96-well plates at a cell density of 4000 cells/well and exposed to a titration of the unconjugated anti-GCC monoclonal antibody or TAK-264 for 96 h. Cell viability was assessed using the WST assay (Roche, Indianapolis, IN), according to manufacturer's directions. Triplicate wells were used for each treatment, and

viability was normalized to untreated cells. Error was calculated as the standard error of the mean (SEM) of three independent experiments.

### Human xenograft tumor studies

All animal research and veterinary care were performed at Takeda Boston, and the study was conducted using a protocol approved by the Takeda Boston Institutional Animal Care and Use Committee (IACUC) in a facility accredited by the Association for Assessment and Accreditation of Laboratory animal Care International (AAALAC). Immunocompromised mice were housed in a controlled environment and received food and water ad libitum.

Six- to seven-week old CB17 SCID female mice were inoculated subcutaneously with  $5 \times 10^6$  of HEK293-GCC cells or human primary tumors in DMEM without 10% FBS medium. For PHTX studies (PHTX-09C, PHTX-21C, PHTX-07C, PHTX-17C, and PHTX-11C), mice were implanted subcutaneously in the right flank with tumor fragments from primary human colon tumor tissue propagated in mice. Tumor growth was monitored using Vernier calipers, and the mean tumor volume was calculated using the formula ( $0.5 \times [\text{length} \times \text{width}^2]$ ).

For *in vivo* pharmacokinetic and pharmacodynamic studies, when the mean tumor volume reached approximately  $500 \text{ mm}^3$ , animals were randomized into treatment groups ( $n = 3$ , TAK-264 treatment group;  $n = 4$ , vehicle group). Mice received a single intravenous dose of vehicle or TAK-264 1.875 or 3.75 mg/kg. The animals were sacrificed at defined time points (1, 4, 8, 24, and 48 h, and 4 days) following a single intravenous administration of TAK-264, and tumor and whole blood samples were harvested. The blood samples were transferred into serum separator tubes (BD#365956).

For *in vivo* activity studies, mice were randomized into treatment groups of 10 mice per group when tumors reached approximately  $200 \text{ mm}^3$ . Mice were dosed intravenously (0.1 mL dosing volume) once-weekly for a total of three doses. The treatment groups included vehicle (0.9% saline), 209-vcMMAE (non-targeting control antibody) at 7.5 and 10 mg/kg, TAK-264 at 1.875, 3.75, 7.5, and 10 mg/kg, and free MMAE at 0.3 mg/kg (toxin equivalent). Tumor growth inhibition was calculated at last day with vehicle control group using the formula ( $\text{control average tumor volume} - \text{treated average tumor volume} \times 100 / \text{control average volume}$ ).

Mice were anesthetized using an isoflurane/oxygen mix and kept under anesthesia while tumor fragments were implanted, and no analgesics were used or required per IACUC guidelines. This method of anesthesia was used due to its short induction and recovery time and the reliability of its effects [34]. There were no unexpected animal deaths due to experimental procedures in the above-mentioned *in vivo* studies. Mice were euthanized using inhaled  $\text{CO}_2$  when the following humane endpoints were reached: tumor volumes reaching  $\geq 10\%$  of the mouse's body weight, tumor length  $\geq 2$  cm, or tumors of any size interfering with eating, drinking, urinating, defecating, or walking. No mice showed any signs illness due tumor formation. Animal health observations were performed twice daily at 10 AM and 3 PM by our husbandry staff. Temperature and relative humidity within the barrier facility rooms were checked (VWR thermometers) and recorded every morning by husbandry staff. The temperature of the rooms was maintained at  $70^\circ\text{F}$ , and temperature fluctuations of  $\pm 2^\circ\text{F}$  degrees were reported to the Animal Facility Supervisor. The relative humidity for animal holding rooms was set to 50%. Any reading more than  $\pm 20\%$  was also immediately reported to the Animal Facility Supervisor. Animals were housed on Alpha Dri<sup>®</sup> or Alpha Dri+<sup>®</sup> bedding with two forms of enrichment (one of which had to be for sheltering or nesting) in Thoren cage setups that had been autoclaved. Water bottles were filled with chlorinated RO water, capped with a neoprene stopper, and then autoclaved in a covered container before placing them on the wire

lid of the Thoren cage. Mice were fed commercially irradiated PicoVac<sup>®</sup> Rodent Diet 20 –Irradiated (#5062). Cage setups as well as bottle water and food were changed once a week (or whenever necessary). All rodent holding rooms were on a ‘12-h on’ (6 AM to 6 PM) and ‘12-h off’ (6 PM to 6 AM) cycle.

### Immunohistochemistry

Detection of phospho-histone H3 was performed on 5 μm-thick, deparaffinized xenograft tumor sections. Slides were incubated for 1 h at 37°C with anti-phospho-histone H3 antibody (Upstate 06–570; 40 μg/mL) diluted in Dako diluents (DAKO USA). Secondary goat anti-rabbit rhodamine-red-X conjugate (Jackson ImmunoResearch 111-295-144; 30 μg/mL) was added for 30 min at room temperature. DAPI Vectashield<sup>®</sup> HardSet<sup>™</sup> medium (Vector Laboratories, Burlingame, CA) was used as a chromatin counterstain. Images were captured with a Nikon Eclipse E800 (20x objective) and analyzed with MetaMorph 6.3r7 software (Molecular Devices, Downingtown, PA).

GCC protein levels in formalin-fixed paraffin-embedded tissues were assessed on 5 μm-thick sections. Slides were incubated with rabbit monoclonal anti-human GCC antibody (Takeda Pharmaceuticals International Co.; 3.5 μg/mL), diluted in Dako diluents (DAKO USA), for 1 h on the Ventana Medical Systems (Tucson, AZ) Discovery XT<sup>®</sup> automated stainer. Antibodies were biotinylated with a rabbit anti-goat secondary antibody (Vector Laboratories) and developed with the 3,3'-diaminobexidine (DAB) substrate map system (Ventana Medical Systems). Slides were counterstained with hematoxylin and imaged using the Aperio whole slide scanning system. Colon tissue microarrays (US Biomax) were stained and scored by two independent pathologists following a protocol developed at Qualtek Molecular Laboratories on their Tek-Mate automated stainer. Briefly, a composite scoring system (0, 1, 2, or 3) was established that captures both staining intensity (negative, weak, moderate, and strong) and the proportion of cells that exhibit the respective staining intensity. This information was used to generate a modified *H*-score that follows the following formula:  $H\text{-score} = (\% \text{ membrane at } 0 + \% \text{ cytoplasm at } 0) \times 0 + (\% \text{ membrane at } 1 + \% \text{ cytoplasm at } 1) \times 1 + (\% \text{ membrane at } 2 + \% \text{ cytoplasm at } 2) \times 2 + (\% \text{ membrane at } 3 + \% \text{ cytoplasm at } 3) \times 3$ . Thus, this score produces a continuous variable that ranges from 0 to 600. Bridging studies were performed to ensure consistency of the data.

### Statistical analysis

One-way ANOVA using the Dunnett's multiple comparison test (GraphPad Prism 5 Software) identified time points with significance.

## Results

### GCC expression is restricted to normal and malignant intestinal epithelial cells

GCC is an intestinal epithelial-selective gene, as demonstrated in a panel of human tissues that was assessed by quantitative RT-PCR (Fig 1A). Analysis of patient-derived tumor samples demonstrated that GCC was detected at the mRNA level in all primary and metastatic CRC tumor samples analyzed (Fig 1B). Using a custom-made GCC-specific rabbit monoclonal antibody, GCC protein expression was assessed in a repository of >300 human CRC tumor samples and normal colon samples by immunohistochemistry. GCC was found to be restricted to the apical surface of normal intestinal epithelial cells facing the lumen (Fig 1C). The staining of primary and metastatic CRC tumor samples demonstrated that GCC was expressed at a score

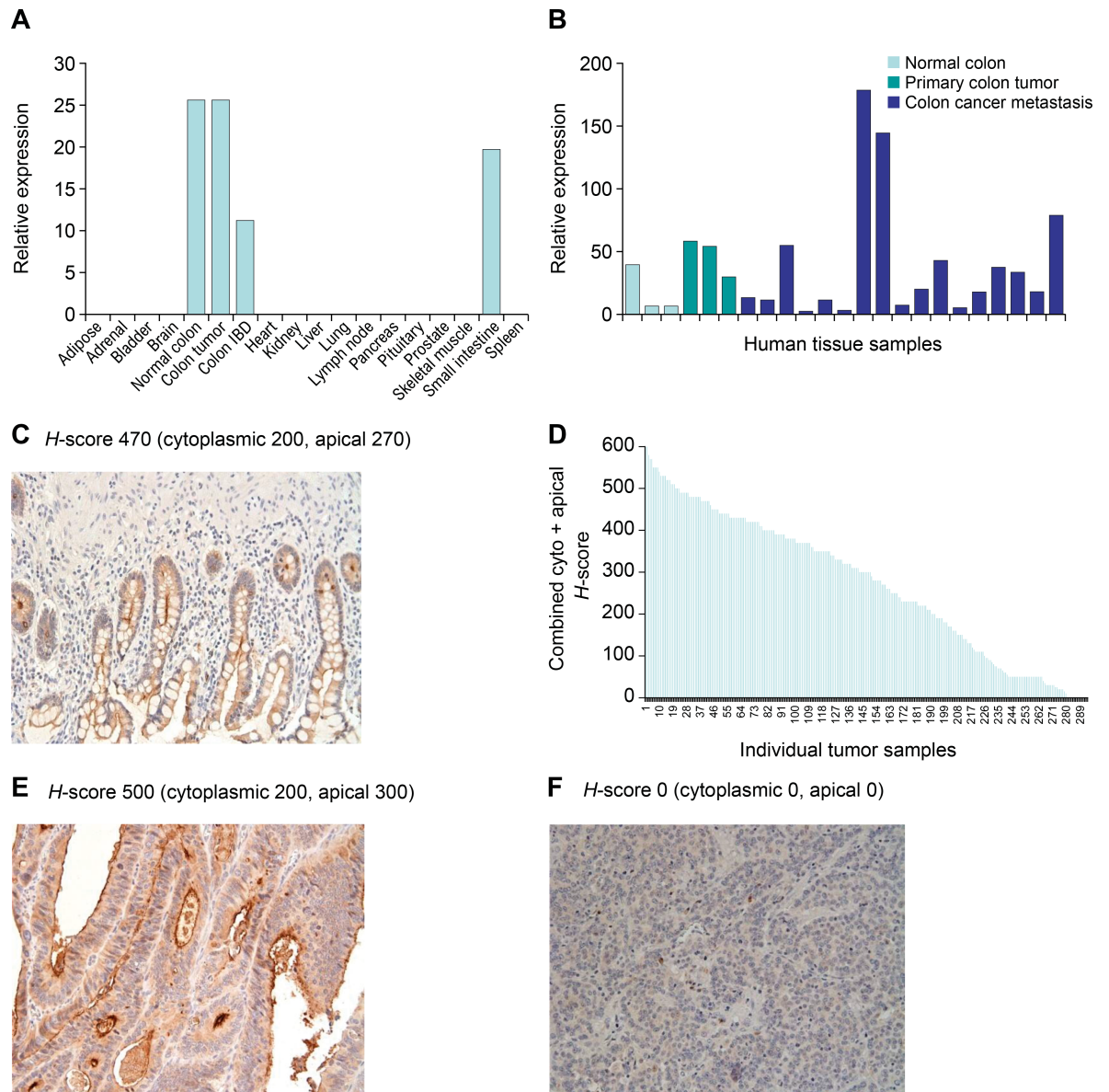


**Fig 1. GCC expression analysis by quantitative RT-PCR and immunohistochemistry.** GCC gene expression was analyzed in (A) a panel of human tissue samples and (B) normal human colon, primary and mCRC cancer samples. (C–F) Expression of GCC in human clinical samples was determined by immunohistochemistry. The intensity of GCC expression was determined by pathologist review and scored according to GCC intensity in the cytoplasm (cyto) and membrane-associated (apical) H-score from 0–300. (C) Expression of GCC in normal colon tissue. (D) A graphical presentation of the combined (cyto + apical) H-score of >300 primary and metastatic colon tumor samples. (E) Expression of GCC in grade 2 metastatic colorectal tumor. (F) Expression of GCC in poorly differentiated metastatic colon tumor. GCC, guanylyl cyclase C; mCRC, metastatic colorectal cancers.

<https://doi.org/10.1371/journal.pone.0191046.g001>

of 50 or more (out of 600) in more than 95% of tumor samples (Fig 1D). The expression pattern fell into two distinct categories; moderately and well-differentiated tumors expressed GCC on an apical surface, while poorly differentiated tumors typically demonstrated a diffuse cytoplasmic staining pattern with varying intensity (Fig 1E and 1F). The restricted expression of GCC at the basement membrane and the tight junctions between intestinal epithelial cells could limit systemically delivered GCC-targeting agents from reaching the gut [24, 35]. In tumor cells, these interactions are disrupted, allowing free access to the antigen, making GCC

one of the most tumor-selective cell surface targets to date, and thus a suitable target for ADC delivery.

### TAK-264 selectively binds, is internalized by, and is cytotoxic to GCC-expressing cells

TAK-264 consists of a fully human anti-GCC monoclonal antibody conjugated to MMAE via the protease-cleavable vc peptide linker [36]. Unconjugated anti-GCC monoclonal antibody and TAK-264 were compared for relative binding to HEK293-GCC, an engineered cell line that was selected for its high level of antigen expression (Fig 2A). TAK-264 and unconjugated anti-GCC monoclonal antibody bound to HEK293-GCC cells in a dose-dependent manner with similar affinities ( $EC_{50}$ : 42 ng/mL and 25 ng/mL, respectively), indicating that conjugation of MMAE to the anti-GCC monoclonal antibody did not significantly affect antigen-binding properties.

Target-dependent internalization of the unconjugated anti-GCC monoclonal antibody and TAK-264 was demonstrated in HEK293-GCC cells using immunofluorescence microscopy with a fluorescently labeled anti-human IgG secondary antibody. When incubated on ice, TAK-264 was strictly localized on the cell surface (Fig 2B, top). Upon incubation at 37°C, punctuate staining was detected intracellularly as early as 15 min (Fig 2B, bottom), indicative of internalization of TAK-264. Unconjugated anti-GCC monoclonal antibody behaved identically to TAK-264 on HEK293-GCC cells (data not shown). No binding or internalization was detected for TAK-264 or the unconjugated anti-GCC monoclonal antibody with HEK293-vector control cells (data not shown). Following binding to GCC, TAK-264 was endocytosed and trafficked to the lysosomes, where MMAE is released by lysosomal proteases [37]. A time-dependent accumulation of MMAE was observed by LC/MS/MS analysis of cell culture supernatant and pellets collected from samples incubated with 1  $\mu$ g TAK-264 at 37°C, 5% CO<sub>2</sub> (Fig 2C).

To evaluate TAK-264 *in vitro* cytotoxicity, HEK293-GCC or HEK293-vector cells were incubated with TAK-264 or unconjugated anti-GCC monoclonal antibody alone (Fig 2D). Unconjugated anti-GCC monoclonal antibody had no effect on HEK293-GCC cell viability. However, TAK-264 potently reduced HEK293-GCC cell viability, with a 50% lethal dose ( $LD_{50}$ ) of 39 pM, approximately 1000-fold lower than the TAK-264  $LD_{50}$  on HEK293-vector cells (42.5 nM), indicating that the cytotoxic activity of TAK-264 is highly target-dependent. The HEK293-GCC and HEK293-vector cells showed similar sensitivity to free MMAE (S1 Table). The cytotoxic activity of TAK-264 was substantially reduced in HT-29 cells engineered to express GCC. Interestingly, this cell line expresses less GCC at the cell surface (S2 Table), indicating that TAK-264 potency is driven at least in part by antigen surface density. We next tested the activity of TAK-264 in GCC-expressing tumor xenografts.

### *In vivo* pharmacodynamics and pharmacokinetics of TAK-264

The anti-tumor activity of TAK-264 was evaluated in engineered HEK293-GCC xenograft tumors as well as in primary human tumor xenografts that had GCC expression patterns closely resembling those found in patient tumor samples. The expression of GCC was validated by immunohistochemistry. GCC levels differed among these tumors (Table 1; Fig 3). In moderate/well-differentiated tumors that maintained a polarized epithelial cellular structure, GCC was concentrated on the luminal side of the tumor tissue.

In order to study the relationship between uptake of antibody, release of MMAE, and the pharmacodynamic effect of TAK-264 in xenograft tumors, we measured the fraction of cells in mitosis, the concentration of free MMAE, and the uptake of radiolabeled monoclonal antibody



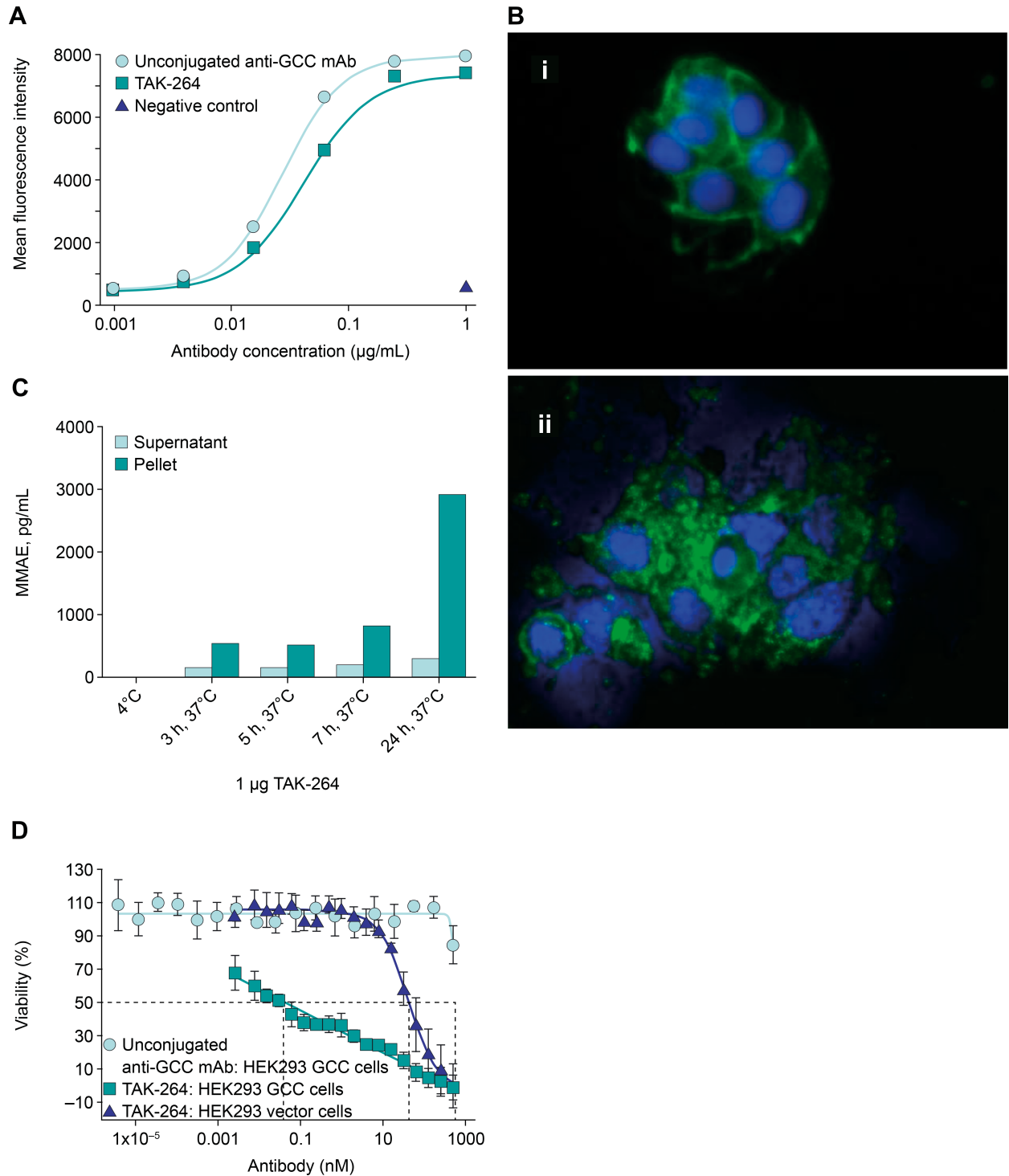


**Fig 2. Characterization of TAK-264 binding, internalization, and *in vitro* cytotoxicity.** (A) Unconjugated anti-GCC monoclonal antibody and TAK-264 bind to GCC-expressing cells. Flow cytometry was performed with unconjugated anti-GCC monoclonal antibody and TAK-264 on HEK293-GCC or HEK293-vector cells. Mean fluorescence intensity is plotted versus monoclonal antibody concentration ranging from 0.001–1 µg/mL. (B) TAK-264 is internalized by GCC-expressing cells. Internalization assays were performed with TAK-264 on HEK-GCC cells. Antibodies were incubated with cells at (i) 4°C for 30 min or at (ii) 37°C for 3 h, prior to fixing and staining with secondary antibody. Immunofluorescence was visualized with a confocal microscope (Zeiss Pascal) and analyzed using Axiovert software. (C) Time-dependent accumulation of MMAE in samples incubated with 1 µg TAK-264 at 37°C, 5% CO<sub>2</sub>, and analyzed by LC/MS/MS. (D) *In vitro* cytotoxicity of TAK-264. Cell viability was assessed 4 days after incubation of HEK293-GCC cells or HEK293-vector cells with increasing concentrations of unconjugated and MMAE-

conjugated anti-GCC monoclonal antibody. The average of three independent experiments is plotted with error represented as SEM. GCC, guanylyl cyclase C; LC/MS/MS, liquid chromatography–tandem mass spectrometry; MMAE, monomethyl auristatin E; SEM, standard error of the mean.

<https://doi.org/10.1371/journal.pone.0191046.g002>

at matched time points. Mice carrying HEK293-GCC or primary human tumor explant (PHTX)-09c tumors were evaluated by immunofluorescence for phospho-histone H3 levels, a mitotic marker, following a single IV dose of TAK-264 at 1.875 or 3.75 mg/kg. There was a time-dependent effect of TAK-264 on the tumor cells (Fig 4) that was consistent with the mechanism of action of MMAE [29, 36]. The fraction of phospho-histone H3-positive cells increased 3- to 4-fold, peaking 3–4 days post-injection. The peak concentration of MMAE delivered to the tumors by TAK-264 coincided with the peak in phospho-histone H3 staining, demonstrating a direct correlation between free MMAE and mitotic arrest. The time to peak MMAE concentrations coincided with peak antibody uptake in the tumors as assessed by single photon emission computed tomography *in vivo* imaging of <sup>111</sup>In-labeled TAK-264 [35].

Hence, there was a correlation between antibody uptake in the tumor, release of MMAE from the ADC, and the effect on the tumor. HEK293-GCC tumors, which show greater GCC expression than PHTX-09c tumors, showed higher concentrations of free MMAE compared with the PHTX-09c tumors, demonstrating the target density-dependent accumulation of cytotoxic payload (S2 Fig).

### ***In vivo* activity of TAK-264 in HEK293-GCC tumor-bearing mice and in PHTX models of mCRC**

Tumor-bearing mice were treated on a once-weekly schedule, for three doses, with vehicle, non-targeting control antibody 209-vcMMAE, free MMAE, or TAK-264 at various doses. In HEK293-GCC tumors (GCC expression H-score of 600 by immunohistochemistry; Fig 5A), treatment with non-targeting ADC (209-vcMMAE) or free MMAE alone had no effect on tumor growth; however, treatment with TAK-264 at 1.875, 3.75, or 7.5 mg/kg resulted in tumor growth inhibition in a dose-dependent fashion; respective TGI values on day 17 (last day control mice remained on study) were 55%, 84%, and 97% ( $P > 0.05$ ,  $P < 0.01$ , and  $P < 0.001$ , respectively). In the PHTX-09c tumor model (GCC expression H-score of 500 by immunohistochemistry), dose-dependent anti-tumor activity was also observed with TAK-264 (Fig 5B); TGI values following treatment with TAK-264 at 3.75, 7.5, and 10 mg/kg were 66%,

**Table 1. Summary of TAK-264 anti-tumor activity in *in vivo* models of GCC-expressing tumor xenografts.**

Model	GCC expression H-score		TAK-264 dose*	T/C at 7.5 mg/kg	P-value	T/C at 10 mg/kg	P-value
	Cytoplasmic	Apical					
HEK293-GCC	300	300	1.875–7.5 mg/kg	0.03	<0.001	NA	NA
PHTX-09c	250	250	0.938–10 mg/kg	0.16	<0.001	0.09	<0.001
PHTX-21c <sup>†</sup>	10	100	3.75–10 mg/kg	0.38	<0.001	0.23	<0.001
PHTX-07c <sup>†</sup>	50	280	3.75–10 mg/kg	0.74	<0.05	0.53	<0.001
PHTX-17c <sup>†</sup>	50	40	0.938–10 mg/kg	0.5	<0.001	0.46	<0.05
PHTX-11c <sup>†</sup>	120	300	7.5 mg/kg	0.63	<0.001	NA	NA

\*Once-weekly schedule, three doses of TAK-264

<sup>†</sup>Included in S1 Fig.

IHC, immunohistochemistry; GCC, guanylyl cyclase C; NA, not applicable; T/C, ratio of tumor size relative to control, calculated on the last day on which control mice remained on study.

<https://doi.org/10.1371/journal.pone.0191046.t001>

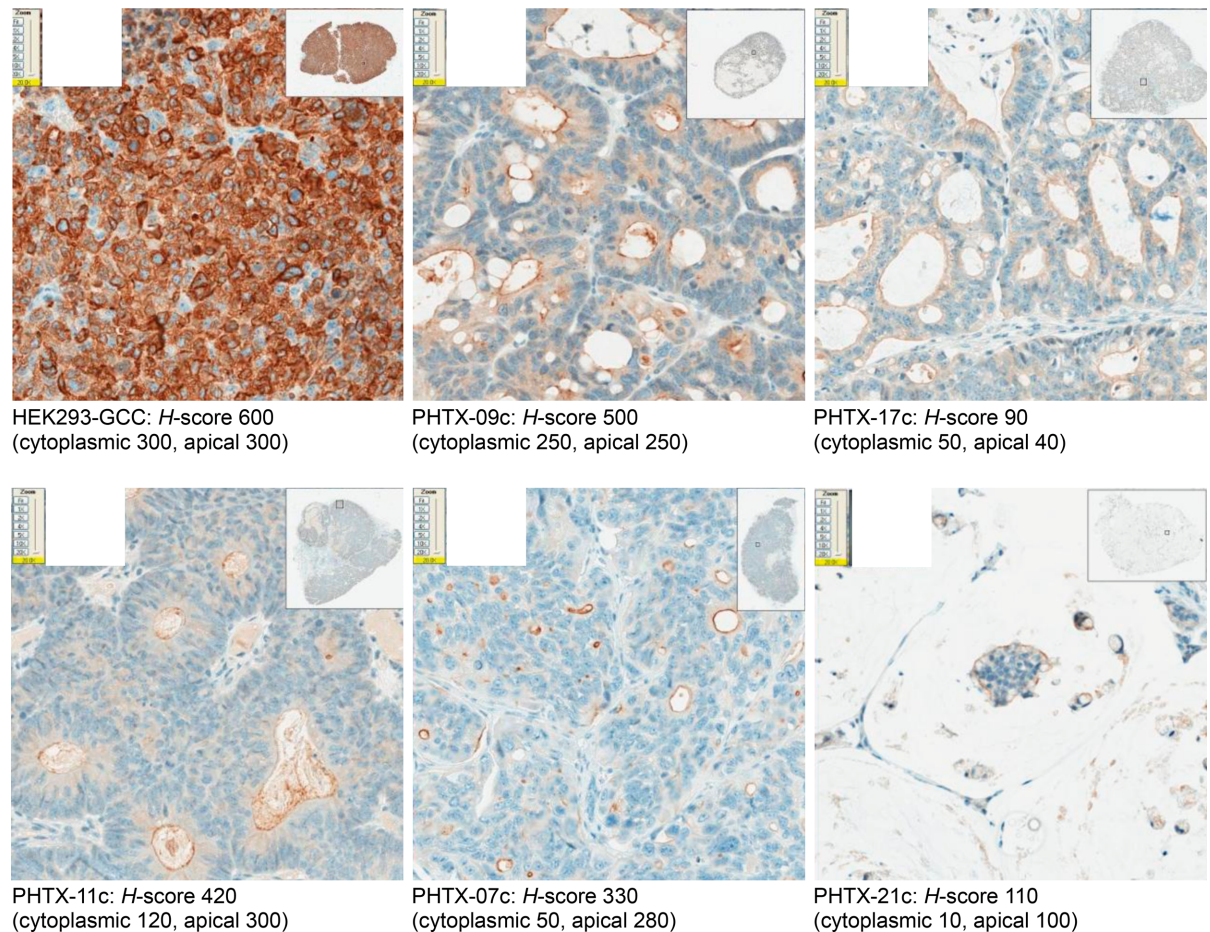


**Fig 3. GCC protein expression in HEK293-GCC and PHTX xenograft tumors (from mCRC patients) in SCID mice. GCC, guanylyl cyclase C.**

<https://doi.org/10.1371/journal.pone.0191046.g003>

84%, and 91%, respectively (all  $P \leq 0.01$ ), on day 20. TAK-264 caused regressions of tumor growth and similar activity in both models although a higher dose was required in PHTX-09c versus HEK293-GCC tumors (10 vs. 7.5 mg/kg).

TAK-264 also demonstrated TGI in other PHTX models (Table 1). Overall, TGI appeared to correlate with antigen density, with tumors with higher GCC expression generally showing greater sensitivity to TAK-264 compared to tumors with lower antigen expression levels. Of particular interest, some models were less sensitive to TAK-264 treatment even though they expressed significant levels of antigen. TAK-264 could be detected at GCC-expressing sites 7 days post-administration of TAK-264, suggesting that the ADC was able to reach GCC-expressing tumor cells (S3 Fig). Furthermore, it is not likely due to a failure of cells to internalize and/or process TAK-264 as levels of free MMAE detected in PHTX-11c, a resistant model, were similar to levels found in the PHTX-09c model following the same dose (data not shown). Drug-efflux pump expression has also been investigated by transcriptional profiling, as MMAE has been demonstrated to be a substrate, particularly for P-glycoprotein [38]; however, no significant differences could be found at the mRNA level between sensitive and resistant PHTX models (data not shown). Thus, these tumors appear inherently resistant to a high local MMAE concentration achieved with TAK-264. The mechanism of MMAE resistance is an ongoing area of investigation.

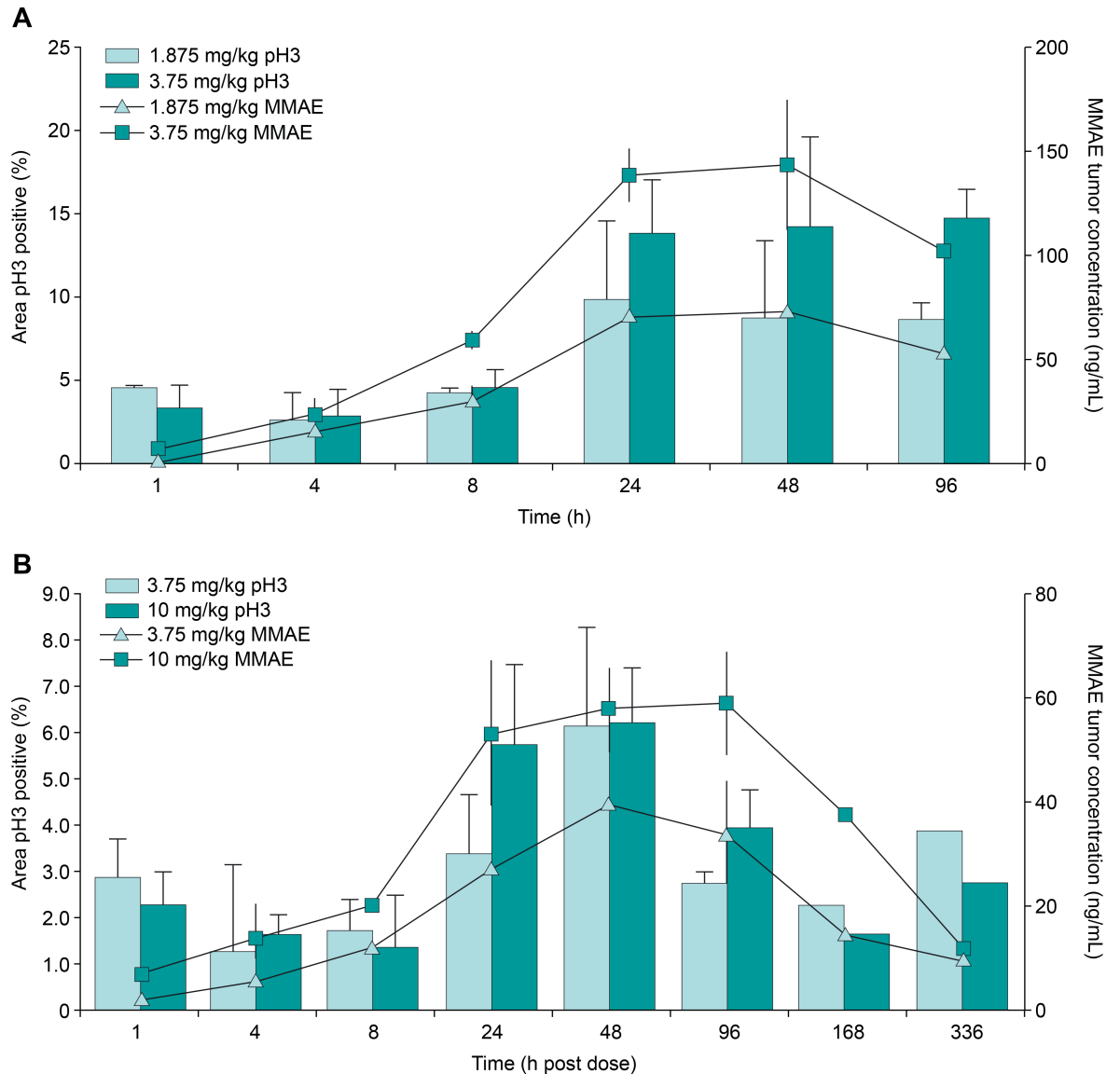


**Fig 4. Phospho-histone H3 and MMAE levels in HEK293-GCC and PHTX-09c xenograft tumors following TAK-264 treatment.** (A) HEK293-GCC and (B) PHTX-09 xenograft tumors were harvested at the indicated times post-treatment, with three animals per time point. Control tumors were taken from three untreated mice. The average percentage of phospho-histone H3-positive cells and average level of MMAE tumor concentration are plotted, with error represented as standard deviation. GCC, guanylyl cyclase C; MMAE, monomethyl auristatin E.

<https://doi.org/10.1371/journal.pone.0191046.g004>

## Discussion

We have herein described the development of an ADC targeted to GCC, which is expressed in >95% of primary and metastatic CRC tumors and in 60–70% of gastric, esophageal, and pancreatic cancers [16, 17, 39]. TAK-264 consists of a fully human anti-GCC monoclonal antibody linked to the highly potent cytotoxic agent MMAE via a protease-cleavable linker (vc; MMAE and the linker technology are licensed from Seattle Genetics, Inc.). TAK-264 retained cell surface binding specificity and affinity comparable to unconjugated anti-GCC monoclonal antibody and was internalized by GCC-expressing cells. TAK-264 demonstrated potent cytotoxicity against HEK293-GCC but not HEK293-vector cells. When administered to mice

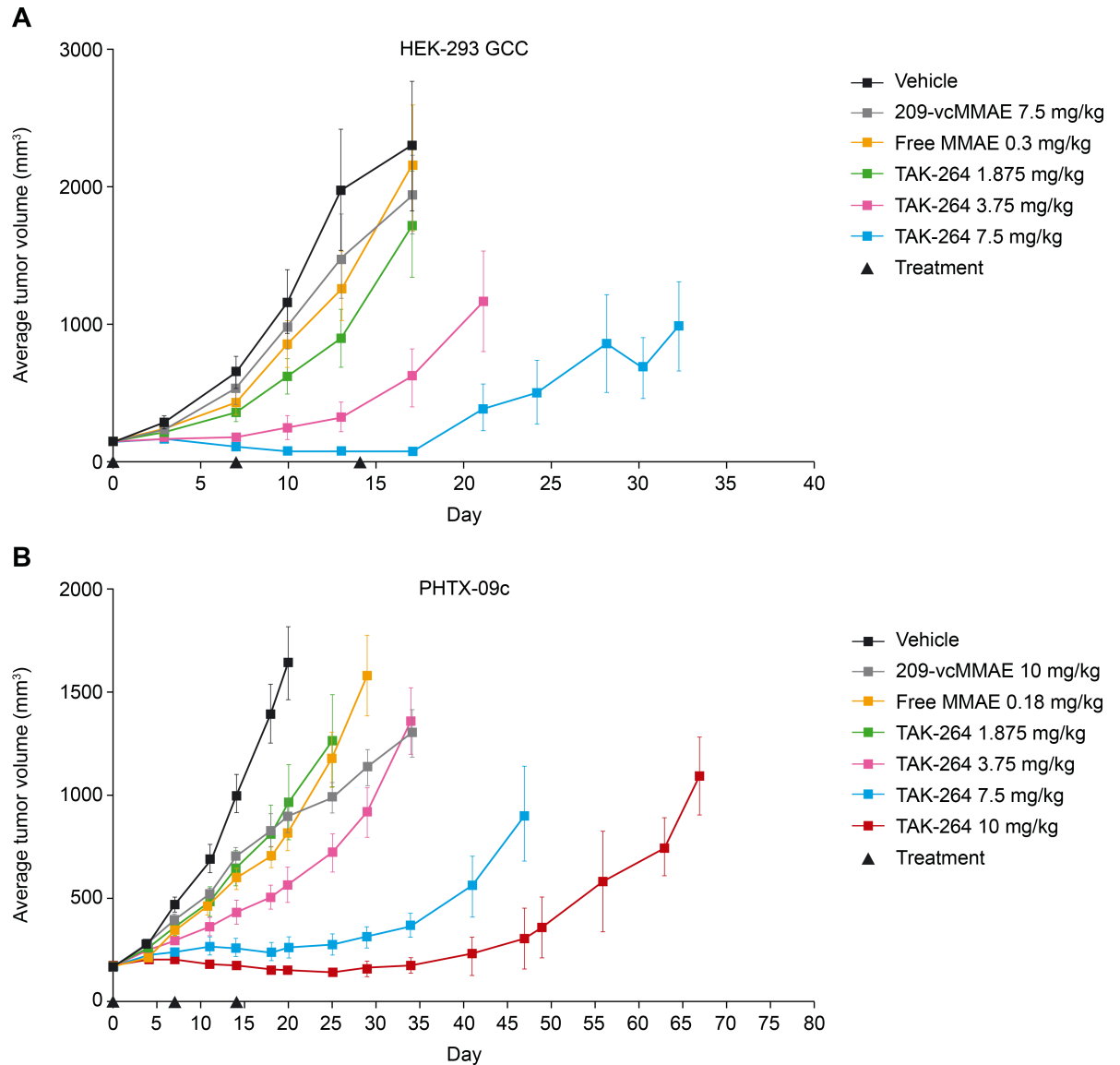


**Fig 5. TAK-264 induces tumor regression and long-term tumor growth delay of GCC-expressing tumors.** Female SCID mice bearing (A) GCC-expressing HEK293 xenograft tumors and (B) PHTX-09c tumors, a patient-derived xenograft model of mCRC, were treated when the tumor reached approximately 200 mm<sup>3</sup> with either vehicle, non-targeting control antibody 209-vcMMAE, free MMAE, or TAK-264 at various doses on a weekly dosing schedule indicated by the black triangles. Average tumor volume was determined at multiple time points following start of treatment and is shown  $\pm$  S.E.M.

<https://doi.org/10.1371/journal.pone.0191046.g005>

bearing GCC-expressing xenografts, which had comparable levels of GCC expression to those observed in human mCRC tissue samples, a single administration of TAK-264 resulted in mitotic arrest from 24 h to 4 days post-injection. This cytotoxicity corresponded to elevated free MMAE levels in tumor tissue, indicating that proteolytic cleavage of TAK-264 occurred following internalization. TAK-264 demonstrated a dose-dependent anti-tumor activity in HEK293-GCC and human primary tumor mouse xenograft models. These data support the clinical development of TAK-264 for the treatment of GCC-expressing tumors.

Pharmacokinetic and pharmacodynamic analyses in HEK293-GCC xenograft mice indicate that TAK-264 is selectively cleaved in GCC-expressing tumor cells, leading to cell death. TAK-



264 appears relatively stable in circulation, with limited release of free MMAE. These observations are consistent with previous studies that have demonstrated high serum stability and efficient targeted hydrolysis of ADCs with protease-cleavable vc-dipeptide linkers [40]. HEK293-GCC xenograft mice tolerated the administered doses of TAK-264 with the schedule tested. Doses of TAK-264 up to 7.5–10 mg/kg on a once-every-3-weeks schedule were required for an anti-tumor effect in mice. This dosing regimen was well-tolerated in all preclinical studies; however, clinical data suggests that this exceeds clinically achievable concentrations. During clinical evaluation of TAK-264, a maximum tolerated dose was determined to be 1.8 mg/kg on a once-every-3-weeks schedule [41], consistent with the maximum tolerated dose for other ADCs with the same linker payload on the same schedule [42, 43].

Many properties of GCC make it an attractive target for the development of an antibody-based therapeutic for mCRC and other GCC-expressing malignancies. The expression pattern is its foremost attribute, with expression restricted to the luminal membrane of normal intestinal tissues (large intestine, small intestine, and rectum) [10, 11] and maintained in primary CRC and mCRC tumors [12–14]. The apical-located GCC in normal intestinal epithelial cells is not in direct contact with the bloodstream [10, 24, 44], and therefore is predicted to be inaccessible by an ADC administered intravenously. In contrast, GCC expression on CRC metastases to the liver becomes less polarized and the tissue structure/vascularity within tumors could allow anti-GCC ADCs to specifically target tumor metastases while sparing normal gastrointestinal tissues. As the unconjugated anti-GCC monoclonal antibody does not cross-react with mouse GCC protein (data not shown), we were not able to test this hypothesis directly. However, rates of gastrointestinal toxicities were generally limited in the first-in-human phase 1 study, with 51% of patients reporting nausea, 49% decreased appetite, 39% diarrhea, and 24% constipation and vomiting; toxicities were generally mild or moderate in severity, with only 7% grade  $\geq 3$  diarrhea [41].

GCC expression in primary and metastatic colon tumor tissues is heterogeneous among patients, as well as within a single tumor. We chose to study TAK-264 activity in PHTX models that more closely resemble human disease and the observed GCC expression pattern. We also assumed that the range of drug levels evaluated in our preclinical experiments would be informative in the context of clinical studies, with the aim of achieving similar antitumor effects as observed in our xenograft models, i.e., TAK-264 would be expected to induce tumor cell death and reduce tumor burden in mCRC patients and other GCC-expressing cancers. Our *in vivo* experiments suggest that TAK-264 cytotoxic activity may be dependent on antigen expression density, as assessed by immunohistochemistry. Determining GCC expression level and how it relates to antitumor activity will be an objective during the clinical development of TAK-264. Furthermore, it will be important to define non-invasive biomarkers to select the appropriate responsive patient population.

Observations in PHTX models suggest that some tumors may be refractory to TAK-264 despite moderate to high GCC expression, possibly suggesting a degree of TAK-264 resistance. The defined mechanism of TAK-264 resistance is an area of ongoing investigation. A study has shown that MMAE is a substrate for some drug pumps [45]. It is possible that over-expression of pumps may render tumors less sensitive to the effects of TAK-264. The spindle checkpoint is an evolutionary conserved mechanism involving several key regulators that monitor fidelity of chromosome separation during mitosis [46]. A number of *in vitro* studies have indicated that dysregulation of key spindle checkpoint regulators compromise the sensitivity of cancer cells to microtubule inhibitors such as paclitaxel and docetaxel [47–50]. This may explain why these agents have failed to demonstrate significant clinical benefit in CRC [46]. Indeed, 80–85% of CRC tumors display chromosomal instability that can sometimes be attributable to expression abnormalities or somatic mutations in spindle checkpoint regulators [51].

In clinical studies, the cancer molecular subtype (chromosomal instability, microsatellite instability phenotype, and CpG island methylator phenotype) and expression levels/mutation status of various genes could be assessed to help identify biomarkers that could stratify patient populations likely to respond to TAK-264.

In summary, we have demonstrated that TAK-264 is cytotoxic *in vitro* and *in vivo* to GCC-expressing cells, providing a solid scientific rationale for further preclinical and clinical development of this drug. As GCC is a highly specific colon epithelial antigen that is expressed on both primary and metastatic CRC tumors as well as gastric, esophageal, and pancreatic tumors, TAK-264 may provide a novel targeted approach for the treatment of these GCC-expressing malignancies, which are diseases of unmet medical need.

## Supporting information

**S1 Table. *In vitro* cytotoxicity of TAK-264 and free MMAE in HEK293-GCC and HEK293--vector cells and in HT29-GCC and HT29-vector cells.** HT29-GCC cells were engineered to express GCC but with fewer GCC molecules per cell compared with HEK293-GCC. (DOCX)

**S2 Table. Relative cell surface expression of GCC in HEK293-GCC and HT29-GCC cells, as measured by fluorescence activated cell sorting (mean fluorescence intensity normalized to control).** (DOCX)

**S1 Fig. TAK-264 activity in GCC-positive PHTX models of colorectal cancer.** (TIF)

**S2 Fig. Pharmacokinetic and pharmacodynamic characteristics of TAK-264 in HEK293-GCC or PHTX-09c tumor-bearing SCID mice.** (TIF)

**S3 Fig. TAK-264 human Ig chain in 7 days post-administration PHTX-09c xenografts localizes to sites of GCC expression in serial sections.** (TIF)

**S1 File. NC3Rs checklist Page 1.** (PDF)

**S2 File. NC3Rs checklist Page 2.** (PDF)

## Acknowledgments

The authors would like to acknowledge the contributions of Alice McDonald and Sam Nam, formerly of Millennium Pharmaceuticals, Inc., a wholly owned subsidiary of Takeda Pharmaceutical Company Limited, for their contributions to the work reported in this manuscript, and the contributions to bioanalysis and TAK-264 pharmacokinetics of Susan Chen and Robert Griffin of Millennium Pharmaceuticals, Inc., a wholly owned subsidiary of Takeda Pharmaceutical Company Limited. The authors also acknowledge Lynn Pritchard and Steve Hill of FireKite, an Ashfield Company, part of UDG Healthcare plc, for writing support in the preparation of this manuscript, which complied with Good Publication Practice 3 ethical guidelines (Battisti *et al. Ann Intern Med.* 2015;163:461–4).

## Author Contributions

**Conceptualization:** Daniel P. Bradley, Edward Greenfield, Mark Manfredi, Brad Stringer, Mark Williamson, Tim Wyant, O. Petter Veiby.

**Data curation:** Julie Zhang, Edward Greenfield, Mark Manfredi, Adnan Abu-Yousif.

**Formal analysis:** Melissa Gallery, Julie Zhang, Daniel P. Bradley, Edward Greenfield, Brad Stringer, Johnny Yang.

**Investigation:** Melissa Gallery, Donna Cvet, Jose Estevam, Hadi Danaee, Edward Greenfield, Huay-Keng Loke, Claudia Rabino, Brad Stringer, Tim Wyant, Johnny Yang, Qing Zhu.

**Methodology:** Melissa Gallery, Julie Zhang, Daniel P. Bradley, Jose Estevam, Edward Greenfield, Claudia Rabino.

**Project administration:** Daniel P. Bradley, Ping Li, Adnan Abu-Yousif, O. Petter Veiby.

**Resources:** Daniel P. Bradley, Pamela Brauer, Ping Li, Huay-Keng Loke, Brad Stringer.

**Supervision:** Daniel P. Bradley, Mark Williamson, O. Petter Veiby.

**Validation:** Julie Zhang.

**Visualization:** Melissa Gallery, Julie Zhang, Brad Stringer, Adnan Abu-Yousif.

**Writing – original draft:** Melissa Gallery, Julie Zhang, Daniel P. Bradley.

**Writing – review & editing:** Daniel P. Bradley, Hadi Danaee, Claudia Rabino, Brad Stringer, Mark Williamson, Tim Wyant, Johnny Yang, Adnan Abu-Yousif, O. Petter Veiby.

## References

1. Siegel RL, Miller KD, Jemal A. Cancer statistics, 2015. *CA Cancer J Clin.* 2015; 65(1):5–29. <https://doi.org/10.3322/caac.21254> PMID: 25559415
2. Mekenkamp LJ, Koopman M, Teerenstra S, van Krieken JH, Mol L, Nagtegaal ID, et al. Clinicopathological features and outcome in advanced colorectal cancer patients with synchronous vs metachronous metastases. *Br J Cancer.* 2010; 103(2):159–64. <https://doi.org/10.1038/sj.bjc.6605737> PMID: 20551951
3. Bengtsson G, Carlsson G, Hafstrom L, Jonsson PE. Natural history of patients with untreated liver metastases from colorectal cancer. *Am J Surg.* 1981; 141(5):586–9. PMID: 7223955
4. Leporrier J, Maurel J, Chiche L, Bara S, Segol P, Launoy G. A population-based study of the incidence, management and prognosis of hepatic metastases from colorectal cancer. *Br J Surg.* 2006; 93(4):465–74. <https://doi.org/10.1002/bjs.5278> PMID: 16523446
5. O'Connell JB, Maggard MA, Ko CY. Colon cancer survival rates with the new American Joint Committee on Cancer sixth edition staging. *J Natl Cancer Inst.* 2004; 96(19):1420–5. <https://doi.org/10.1093/jnci/djh275> PMID: 15467030
6. Davies JM, Goldberg RM. Treatment of metastatic colorectal cancer. *Semin Oncol.* 2011; 38(4):552–60. <https://doi.org/10.1053/j.seminoncol.2011.05.009> PMID: 21810514
7. Manfredi S, Lepage C, Hatem C, Coatmeur O, Faivre J, Bouvier AM. Epidemiology and management of liver metastases from colorectal cancer. *Ann Surg.* 2006; 244(2):254–9. <https://doi.org/10.1097/01.sla.0000217629.94941.cf> PMID: 16858188
8. Seicean A, Petrusel L, Seicean R. New targeted therapies in pancreatic cancer. *World J Gastroenterol.* 2015; 21(20):6127–45. <https://doi.org/10.3748/wjg.v21.i20.6127> PMID: 26034349
9. Han X, Mann E, Gilbert S, Guan Y, Steinbrecher KA, Montrose MH, et al. Loss of guanylyl cyclase C (GCC) signaling leads to dysfunctional intestinal barrier. *PLoS One.* 2011; 6(1):e16139. <https://doi.org/10.1371/journal.pone.0016139> PMID: 21305056
10. Carrithers SL, Parkinson SJ, Goldstein SD, Park PK, Urbanski RW, Waldman SA. Escherichia coli heat-stable enterotoxin receptors. A novel marker for colorectal tumors. *Dis Colon Rectum.* 1996; 39(2):171–81. PMID: 8620784
11. Camci C, Sahin A, Sevinc A, Kalender ME, Oztuzcu S, Sever ON, et al. Peripheral blood guanylyl cyclase c (GCC) expressions are associated with prognostic parameters and response to therapy in

- colorectal cancer patients. *Tumour Biol.* 2011; 32(6):1265–70. <https://doi.org/10.1007/s13277-011-0231-0> PMID: 21901559
12. Carrithers SL, Parkinson SJ, Goldstein S, Park P, Robertson DC, Waldman SA. Escherichia coli heat-stable toxin receptors in human colonic tumors. *Gastroenterology.* 1994; 107(6):1653–61. PMID: 7958675
  13. Winn B, Tavares R, Matoso A, Noble L, Fanion J, Waldman SA, et al. Expression of the intestinal biomarkers Guanylyl cyclase C and CDX2 in poorly differentiated colorectal carcinomas. *Hum Pathol.* 2010; 41(1):123–8. <https://doi.org/10.1016/j.humpath.2009.07.009> PMID: 19800103
  14. Buc E, Vartanian MD, Darcha C, Dechelotte P, Pezet D. Guanylyl cyclase C as a reliable immunohistochemical marker and its ligand Escherichia coli heat-stable enterotoxin as a potential protein-delivering vehicle for colorectal cancer cells. *Eur J Cancer.* 2005; 41(11):1618–27. <https://doi.org/10.1016/j.ejca.2005.02.031> PMID: 15919201
  15. John M, Wiedenmann B, Kruhoffer M, Adermann K, Ankorina-Stark I, Schlatter E, et al. Guanylin stimulates regulated secretion from human neuroendocrine pancreatic cells. *Gastroenterology.* 1998; 114(4):791–7. PMID: 9516400
  16. Kloeters O, Friess H, Giese N, Buechler MW, Cetin Y, Kulaksiz U. Uroguanylin inhibits proliferation of pancreatic cancer cells. *Scand J Gastroenterol.* 2008; 43(4):447–55. <https://doi.org/10.1080/00365520701746378> PMID: 18365910
  17. Park J, Schulz S, Haaf J, Kairys JC, Waldman SA. Ectopic expression of guanylyl cyclase C in adenocarcinomas of the esophagus and stomach. *Cancer Epidemiol Biomarkers Prev.* 2002; 11(8):739–44. PMID: 12163327
  18. Schulz S, Hyslop T, Haaf J, Bonaccorso C, Nielsen K, Witek ME, et al. A validated quantitative assay to detect occult micrometastases by reverse transcriptase-polymerase chain reaction of guanylyl cyclase C in patients with colorectal cancer. *Clin Cancer Res.* 2006; 12(15):4545–52. <https://doi.org/10.1158/1078-0432.CCR-06-0865> PMID: 16899600
  19. Sargent DJ, Resnick MB, Meyers MO, Goldar-Najafi A, Clancy T, Gill S, et al. Evaluation of guanylyl cyclase C lymph node status for colon cancer staging and prognosis. *Ann Surg Oncol.* 2011; 18(12):3261–70. <https://doi.org/10.1245/s10434-011-1731-2> PMID: 21533822
  20. Chang C, Marszlowicz G, Waldman Z, Li P, Snook AE, Lin JE, et al. Guanylyl cyclase C as a biomarker for targeted imaging and therapy of metastatic colorectal cancer. *Biomark Med.* 2009; 3(1):33–45. <https://doi.org/10.2217/17520363.3.1.33> PMID: 20477494
  21. Almenoff JS, Williams SI, Scheving LA, Judd AK, Schoolnik GK. Ligand-based histochemical localization and capture of cells expressing heat-stable enterotoxin receptors. *Mol Microbiol.* 1993; 8(5):865–73. PMID: 8102772
  22. Guarino A, Cohen MB, Overmann G, Thompson MR, Giannella RA. Binding of E. coli heat-stable enterotoxin to rat intestinal brush borders and to basolateral membranes. *Dig Dis Sci.* 1987; 32(9):1017–26. PMID: 3304888
  23. Gali H, Sieckman GL, Hoffman TJ, Owen NK, Mazuru DG, Forte LR, et al. Chemical synthesis of Escherichia coli ST(h) analogues by regioselective disulfide bond formation: biological evaluation of an (111)In-DOTA-Phe(19)-ST(h) analogue for specific targeting of human colon cancers. *Bioconjug Chem.* 2002; 13(2):224–31. PMID: 11906259
  24. Wolfe HR, Mendizabal M, Lleong E, Cuthbertson A, Desai V, Pullan S, et al. In vivo imaging of human colon cancer xenografts in immunodeficient mice using a guanylyl cyclase C—specific ligand. *J Nucl Med.* 2002; 43(3):392–9. PMID: 11884500
  25. Snook AE, Stafford BJ, Li P, Tan G, Huang L, Birbe R, et al. Guanylyl cyclase C-induced immunotherapeutic responses opposing tumor metastases without autoimmunity. *J Natl Cancer Inst.* 2008; 100(13):950–61. <https://doi.org/10.1093/jnci/djn178> PMID: 18577748
  26. Urbanski R, Carrithers SL, Waldman SA. Internalization of E. coli ST mediated by guanylyl cyclase C in T84 human colon carcinoma cells. *Biochim Biophys Acta.* 1995; 1245(1):29–36. PMID: 7654763
  27. Ledford H. Toxic antibodies blitz tumours. *Nature.* 2011; 476(7361):380–1. <https://doi.org/10.1038/476380a> PMID: 21866131
  28. Teicher BA, Chari RV. Antibody conjugate therapeutics: challenges and potential. *Clin Cancer Res.* 2011; 17(20):6389–97. <https://doi.org/10.1158/1078-0432.CCR-11-1417> PMID: 22003066
  29. Younes A, Bartlett NL, Leonard JP, Kennedy DA, Lynch CM, Sievers EL, et al. Brentuximab vedotin (SGN-35) for relapsed CD30-positive lymphomas. *N Engl J Med.* 2010; 363(19):1812–21. <https://doi.org/10.1056/NEJMoa1002965> PMID: 21047225
  30. Younes A, Gopal AK, Smith SE, Ansell SM, Rosenblatt JD, Savage KJ, et al. Results of a Pivotal Phase II Study of Brentuximab Vedotin for Patients With Relapsed or Refractory Hodgkin's Lymphoma. *J Clin Oncol.* 2012; 30(18):2183–9. <https://doi.org/10.1200/JCO.2011.38.0410> PMID: 22454421

31. Lorusso PM, Weiss D, Guardino E, Girish S, Sliwkowski MX. Trastuzumab emtansine: a unique antibody-drug conjugate in development for human epidermal growth factor receptor 2-positive cancer. *Clin Cancer Res.* 2011; 17(20):6437–47. <https://doi.org/10.1158/1078-0432.CCR-11-0762> PMID: 22003071
32. Mack F, Ritchie M, Sapra P. The next generation of antibody drug conjugates. *Semin Oncol.* 2014; 41(5):637–52. <https://doi.org/10.1053/j.seminoncol.2014.08.001> PMID: 25440608
33. Kohler G, Milstein C. Continuous cultures of fused cells secreting antibody of predefined specificity. 1975. *Journal of immunology (Baltimore, Md: 1950).* 2005; 174(5):2453–5. Epub 2005/02/25
34. Gargiulo S, Greco A, Gramanzini M, Esposito S, Affuso A, Brunetti A, et al. Mice anesthesia, analgesia, and care, Part I: anesthetic considerations in preclinical research. *ILAR journal.* 2012; 53(1):E55–69. Epub 2013/02/06 <https://doi.org/10.1093/ilar.53.1.55> PMID: 23382271
35. Cvet D, Orcutt K, Rusckowski M, Cheng D, Robertson R, Veiby P, et al. SPECT imaging of GCC, guanylyl cyclase C, in primary human colorectal explants/grafts and GCC over expressing xenograft cell line derived using 111In-5F9 IgG and 111In-5F9 IgG antibody drug conjugate. *Proceedings of the World Molecular Imaging Congress.* 2011; 2011:P809.
36. Francisco JA, Cerveny CG, Meyer DL, Mixan BJ, Klussman K, Chace DF, et al. cAC10-vcMMAE, an anti-CD30-monomethyl auristatin E conjugate with potent and selective antitumor activity. *Blood.* 2003; 102(4):1458–65. <https://doi.org/10.1182/blood-2003-01-0039> PMID: 12714494
37. Okeley NM, Miyamoto JB, Zhang X, Sanderson RJ, Benjamin DR, Sievers EL, et al. Intracellular activation of SGN-35, a potent anti-CD30 antibody-drug conjugate. *Clin Cancer Res.* 2010; 16(3):888–97. <https://doi.org/10.1158/1078-0432.CCR-09-2069> PMID: 20086002
38. de Claro RA, McGinn K, Kwitkowski V, Bullock J, Khandelwal A, Habtemariam B, et al. U.S. Food and Drug Administration approval summary: brentuximab vedotin for the treatment of relapsed Hodgkin lymphoma or relapsed systemic anaplastic large-cell lymphoma. *Clin Cancer Res.* 2012; 18(21):5845–9. <https://doi.org/10.1158/1078-0432.CCR-12-1803> PMID: 22962441
39. Mao ZB, Zhang JF, Xu Z, Zhu HJ, Zhang JG, Pan ZP, et al. Ectopic expression of guanylyl cyclase C in gastric cancer as a potential biomarker and therapeutic target. *J Dig Dis.* 2009; 10(4):272–85. <https://doi.org/10.1111/j.1751-2980.2009.00396.x> PMID: 19906106
40. Sanderson RJ, Hering MA, James SF, Sun MM, Doronina SO, Siadak AW, et al. In vivo drug-linker stability of an anti-CD30 dipeptide-linked auristatin immunoconjugate. *Clin Cancer Res.* 2005; 11(2 Pt 1):843–52.
41. Almhanna K, Kalebic T, Cruz C, Faris JE, Ryan DP, Jung JA, et al. Phase I study of the investigational anti-guanylyl cyclase antibody-drug conjugate TAK-264 (MLN0264) in adult patients with advanced gastrointestinal malignancies. *Clin Cancer Res.* 2016.
42. Younes A, Bartlett NL, Leonard JP, Kennedy DA, Lynch CM, Sievers EL, et al. Brentuximab vedotin (SGN-35) for relapsed CD30-positive lymphomas. *N Engl J Med.* 2010; 363(19):1812–21. <https://doi.org/10.1056/NEJMoa1002965> PMID: 21047225
43. Bendell J, Saleh M, Rose AA, Siegel PM, Hart L, Sirpal S, et al. Phase I/II study of the antibody-drug conjugate glembatumumab vedotin in patients with locally advanced or metastatic breast cancer. *J Clin Oncol.* 2014; 32(32):3619–25. Epub 2014/10/01 <https://doi.org/10.1200/JCO.2013.52.5683> PMID: 25267761
44. Frick GS, Pitari GM, Weinberg DS, Hyslop T, Schulz S, Waldman SA. Guanylyl cyclase C: a molecular marker for staging and postoperative surveillance of patients with colorectal cancer. *Expert Rev Mol Diagn.* 2005; 5(5):701–13. <https://doi.org/10.1586/14737159.5.5.701> PMID: 16149873
45. O'Brien C, Cavet G, Pandita A, Hu X, Haydu L, Mohan S, et al. Functional genomics identifies ABCC3 as a mediator of taxane resistance in HER2-amplified breast cancer. *Cancer Res.* 2008; 68(13):5380–9. <https://doi.org/10.1158/0008-5472.CAN-08-0234> PMID: 18593940
46. Swanton C, Tomlinson I, Downward J. Chromosomal instability, colorectal cancer and taxane resistance. *Cell Cycle.* 2006; 5(8):818–23. <https://doi.org/10.4161/cc.5.8.2682> PMID: 16628000
47. Anand S, Penrhyn-Lowe S, Venkitaraman AR. AURORA-A amplification overrides the mitotic spindle assembly checkpoint, inducing resistance to Taxol. *Cancer Cell.* 2003; 3(1):51–62. PMID: 12559175
48. Ganguly A, Yang H, Pedroza M, Bhattacharya R, Cabral F. Mitotic Centromere-associated Kinesin (MCAK) Mediates Paclitaxel Resistance. *J Biol Chem.* 2011; 286(42):36378–84. <https://doi.org/10.1074/jbc.M111.296483> PMID: 21903575
49. Masuda A, Maeno K, Nakagawa T, Saito H, Takahashi T. Association between mitotic spindle checkpoint impairment and susceptibility to the induction of apoptosis by anti-microtubule agents in human lung cancers. *Am J Pathol.* 2003; 163(3):1109–16. [https://doi.org/10.1016/S0002-9440\(10\)63470-0](https://doi.org/10.1016/S0002-9440(10)63470-0) PMID: 12937152



50. Sudo T, Nitta M, Saya H, Ueno NT. Dependence of paclitaxel sensitivity on a functional spindle assembly checkpoint. *Cancer Res.* 2004; 64(7):2502–8. PMID: [15059905](#)
51. Migliore L, Migheli F, Spisni R, Coppede F. Genetics, cytogenetics, and epigenetics of colorectal cancer. *J Biomed Biotechnol.* 2011; 2011:792362. <https://doi.org/10.1155/2011/792362> PMID: [21490705](#)